

Synthesis, Characterization of Polypyrrole/Titania/GO by Co-Precipitation Method

Azad Kumar*, Gajanan Pandey

Department of Applied Chemistry, School for Physical sciences, Babasaheb Bhimrao Ambedkar University, Lucknow, Uttar Pradesh, India

ABSTRACT

Nowadays, nanocomposites are a special class of materials having unique physical properties and wide application potential in diverse areas. The present research work describes a proficient method for synthesis of polypyrrole/titanium dioxide (PPy/TiO₂) nanocomposites. These nanocomposites were prepared by one-step in situ deposition oxidative polymerization of pyrrole sulphuric acid using ammonium per sulphate as an oxidant in the presence of ultra fine grade powder of anatase TiO₂ nanoparticles cooled in an ice bath. The obtained nanocomposites were characterized by XRD, TEM, UV-Vis, Fourier-transform infrared (FTIR), X-ray diffraction (XRD) and scanning electron microscope (SEM) techniques. The obtained results showed that TiO₂ nanoparticles have been encapsulated by PPy with a strong effect on the morphology of PPy/TiO₂ nanocomposites.

Keywords : PPy/TiO₂, XRD, SEM, TEM

I. INTRODUCTION

Recently, the progress of conducting polymers such as polyaniline, PPy and polythiophene have drawn the interest of scientists, because of the flexibility of their applications, stability in air, high electrical conductivity, and easy synthesis and polymerization.^[1-4]

Conducting polymers can be prepared by chemical or electrochemical polymerization. In the chemical polymerization process, monomers are oxidized by oxidizing agents or catalysts to produce conducting polymers. The advantage of chemical synthesis is that it offers mass production at reasonable cost. On the other hand, the electrochemical method involves the direct formation of conducting polymers with better control of polymer film thickness and morphology, which makes them suitable for use in electronic devices.^[5, 6] Therefore, the physical and chemical properties of conducting polymers are considerably

dependent upon the dopant and polymerization conditions.

PPy is a conductive polymer with a conjugated-electron backbone that displays unusual electronic properties and uses in batteries, Supercapacitor, electrochemical (bio) sensors, conductive textiles and fabrics, mechanical actuators, electromagnetic interference shielding, antistatic coating, and drug delivery systems.^[7-10] However, the principal problems with the practical utilization of conducting polymers like PPy include its poor mechanical properties like brittleness and low processibility. Nanocomposites are a special class of materials having unique physical properties and wide application potential in diverse areas. Novel properties of nanocomposites can be obtained by the successful combination of the characteristics of parent constituents into a single material. Encapsulation of inorganic nanoparticles inside the shell of conducting polymers is the most popular and interesting aspect of

nanocomposites synthesis. These materials differ from both the pure polymers and the inorganic nanoparticles in some of the physical and chemical properties.^[11,12]

Conducting polymer–inorganic oxide nanocomposites have recently attracted great attention owing to their unique microstructure, outstanding physiochemical and electro-optical properties and wide range of potential uses as a battery cathode and also in constructing nanoscopic assemblies in sensors and microelectronics.^[13, 14]

Titanium dioxide (TiO₂) is an important inorganic material in preparing conducting polymer composites because of its excellent physical and chemical properties, as well as extensive applications in diverse areas, such as coatings, solar cells, and photocatalysts ^[15,16]

This present research work describes an efficient method to synthesize and characterization of PPy/TiO₂ nanocomposites by one-step in situ polymerization of pyrrole. TiO₂ nanoparticles with an average diameter about 15 nm were used as a dopant of PPy. The characteristics of the molecular structure, crystallinity, electrical properties, thermal stability, and morphology of the PPy/TiO₂ nanocomposites are also discussed.^[17-21]

II. EXPERIMENTAL SECTION

Materials

Pyrrole monomer, having molar mass of 67.0 g/mol and density of 0.97 g/cm³, was purchased from Merck and triply distilled until a colourless liquid was obtained. The distilled pyrrole was stored at lower than 5 °C in the absence of light. TiO₂ nanoparticles with an average particle size of 50 nm were prepared. All other chemicals were reagent grade or purer.

Preparation of PPy

1.727 ml pyrrole was dissolved in 50 ml of de-ionized water and stirred for 15 min using a magnetic stirrer.

2.717 ml H₂SO₄ was added slowly from drop to the pyrrole monomer solution. 2.28 g ammonium per sulphate was dissolved in 50 ml of de-ionised water and slowly added drop by drop for half an hour from a burette vertically to the above prepared solution. After stirring for 4 h, the solution was filtered and the residual was washed with double distilled water, methanol and acetone and then dried in an oven at 60 °C. Subsequently, the product is grinded to get powder of PPy.^[22-25]

Preparation of PPy/TiO₂ nanocomposites

3.454 ml pyrrole and 5.434 ml H₂SO₄ were stirred with 100 ml double distilled water and further with 1.036 g TiO₂ with respect to the pyrrole. 4.56 g ammonium per sulphate was dissolved in 100 ml of de-ionized water and slowly added drop by drop for half an hour from a burette vertically to the above prepared solution. After stirring for 4 h, the solution was filtered and the residual was washed with double distilled water, methanol and acetone and then dried in an oven at 60 °C. It was grinded into powder.^[26-27]

Preparation of PPy/TiO₂/GO nanocomposites

3.454 ml pyrrole and 5.434 ml H₂SO₄ were stirred with double distilled water and further with 1.0362 g TiO₂ with respect to the pyrrole. 4.56 g ammonium per sulphate was dissolved in 100 ml of de-ionized water and mixed with 60 mg graphene dioxide and slowly added drop by drop for half an hour from a burette vertically to the above prepared solution. After stirring for 4 h, the solution was filtered and the residual was washed with double distilled water, methanol and acetone, and then dried in an oven at 90 °C. It was grinded into powder.^[28-31]

Characterizations

X-ray diffraction (XRD) patterns of neat TiO₂, PPy, and PPy/TiO₂ nanocomposites were measured in the range of 2θ = 20-80°. Fourier-transform infrared (FTIR) spectra of pristine TiO₂, PPy and PPy/TiO₂ nanocomposites were recorded. The size of TiO₂ particles was investigated with transmission electron microscope (TEM). The morphology of neat

TiO₂, PPy and PPy/TiO₂ nanocomposites was investigated by scanning electron microscopy.

III. RESULTS AND DISCUSSION

XRD patterns of nanocomposites

XRD patterns of pure TiO₂, PPy, PPy/TiO₂ and the PPy/TiO₂/GO synthesized nanocomposites are presented in Figure 1. The broad peak in the region of $2\theta = 20-30^\circ$ in XRD pattern of pure PPy (Figure 1(b)) shows that the synthesized PPy in the absence of TiO₂ nanoparticles is amorphous. Also, the main diffraction peaks of pure TiO₂ nanoparticles are appeared at 25° , 38° , 48° , 54.2° , 57.3° , 64.2° and 69.4° (Figure 1(a)). It can be seen from curves (Figure 1(c)) that the main peaks of PPy/TiO₂ nanocomposites are similar to those of neat TiO₂ nanoparticles. XRD patterns of PPy/TiO₂ nanocomposites show that the broad weak diffraction peak of PPy still exists, but its intensity has been decreased. It implies that when pyrrole is polymerized on TiO₂, each phase maintains his initial structure. The Figure 1(d) shows the XRD pattern of PPy/TiO₂/GO. It is the similar to the XRD pattern of PPy/TiO₂ of nanocomposites. The change occurs in the peak intensity, it implies that the nanocomposite of PPy/TiO₂ deposited on the surface of graphene oxide. There is no bond formation was observed with graphene oxide. The mean size of TiO₂ nanoparticles and PPy/TiO₂ and PPy/TiO₂/GO nanocomposites was observed in nanodimension with Scherrer's calculations.^[28-29]

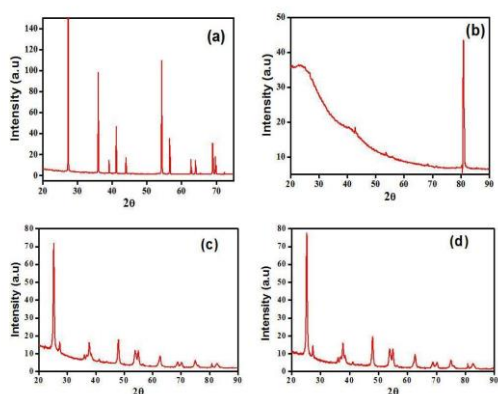


Figure 1. X-Ray diffraction of (a) TiO₂ (b) Pure PPy (c) PPy/TiO₂ (d) PPy/TiO₂/GO

Transmission Electron Microscopy (TEM)

TEM analysis of nanocomposites gives the size and shape of the particles on the scale of atomic diameters. Figure 2 shows the TEM image of TiO₂, PPy, polypyrrole/TiO₂ and polypyrrole/ TiO₂/ GO prepared by Co precipitated method of synthesis. It is observed that the particles are found in the 100 nm range, and are mostly of tetrahedral shape crystals showing in Figure 2(a). The particles size of pure PPy was found in 100 nm range and it is the spiral shape structure of polypyrrole and this is showing in Figure 2(b). The particles size of PPy/TiO₂ was found in 100 nm and it is the observed that the crystals of Titania deposited on the surface of pure polypyrrole.^[30]

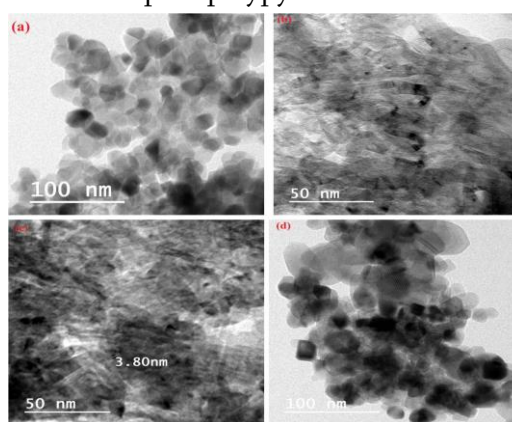


Figure 2. TEM of (a) TiO₂ (b) Pure PPy (c) PPy/TiO₂ (d) PPy/TiO₂/GO

FTIR spectra of Nanocomposites

The FTIR spectra of pure TiO₂, PPy, PPy/TiO₂ and PPy/TiO₂/GO nanocomposites are shown in Figure 3. The spectrum of pure TiO₂ shows one major band at 666 cm^{-1} and a weak peak at 1627 cm^{-1} in the $400-2000\text{ cm}^{-1}$ range. The FTIR spectrum of pure PPy powder prepared with the Ammonium per sulphate oxidant [Figure 3 shows that characteristic band around 1538 and 1463 cm^{-1} correspond to the C=C and C-N stretching modes, respectively. The bands at 1287 and 1044 cm^{-1} are related to the in-plane vibrations of C-H, and strong bands near 1175 and 919 cm^{-1} indicate the doping state of PPy.^[31] The FTIR spectrum of PPy/TiO₂ nanocomposite [Figure 3 is similar of the PPy spectrum, which shows that PPy chains have been formed in the nanocomposites. The FTIR spectrum of PPy/TiO₂/GO nanocomposite

[Figure 3 is similar of the PPy spectrum, which shows that PPy chains have been formed in the nanocomposites. However, the incorporation of TiO₂ leads to the obvious shift of some FTIR bands of PPy.^[32]

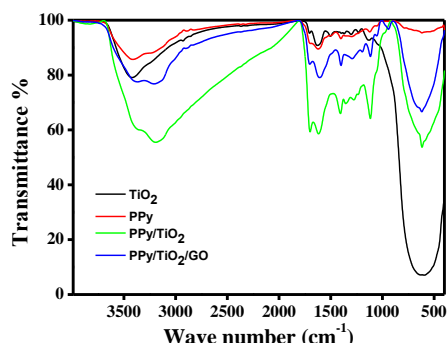


Figure 3. FTIR spectra of TiO₂, pure PPy, PPy/TiO₂ and PPy/TiO₂/GO

SEM of nanocomposites

The morphology and shape of pure TiO₂ nanoparticles, neat PPy, PPy/TiO₂ and PPy/TiO₂/GO nanocomposites were characterized by SEM instrument and the obtained pictures are shown in Figure 4. Figure 4(a) shows that the morphology of pure polypyrrole which is coagulated, disc shaped and nanometric dimensions. As shown in Figure 4(b), TiO₂ nanoparticles were aggregated due to their high surface energy. At low content of TiO₂ (0.025 g TiO₂) is much similar to that of neat PPy and morphology of composites appears as nanoparticles. It indicates that the TiO₂ nanoparticles have a nucleus effect on the pyrrole polymerization and caused a homogeneous PPy shell around them. The SEM images help us draw a conclusion that the doping of TiO₂ has a strong effect on PPy morphology and with the increase of TiO₂ contents, the composites show a transformation in morphology from typical PPy to nanoparticles.^[33]

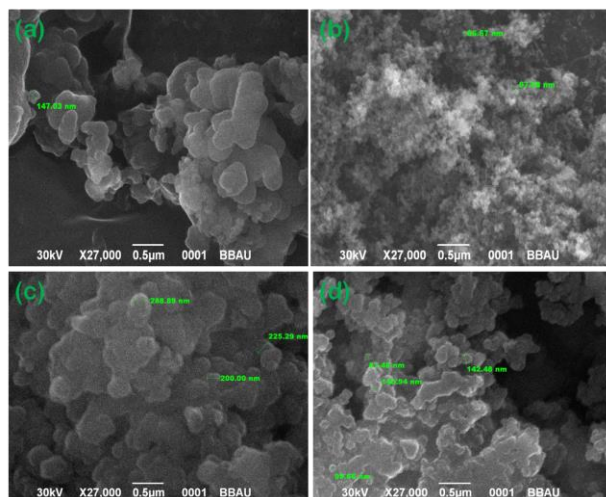


Figure 4. SEM images of (a) pure PPy, (b) pure TiO₂, (c) PPy/TiO₂ (d) PPy/TiO₂/GO nanocomposites.

UV-Visible Spectra

Figure 6(a) showing the UV spectra of TiO₂ nanoparticles, the peak observed between 200-300 nm. Figure 6(b) shows the UV spectra of polypyrrole, the peak observed between 250-300 nm. Figure 6(c) displays the UV spectra of PPy/TiO₂, the peak observed between 200-300 nm. It can be clearly seen that the absorbance range from 200-300 nm due to presence of pyrrole ring. The visible light absorbance of PPy/TiO₂ increase, to associate with PPy content on the surface of TiO₂ nanoparticles. Figure 6(d) displays UV visible spectra of PPy/TiO₂/GO nanocomposites, two peaks are observed in the range of 300 nm and between 400-500 nm due to presence of pyrrole ring and graphene oxide [34].

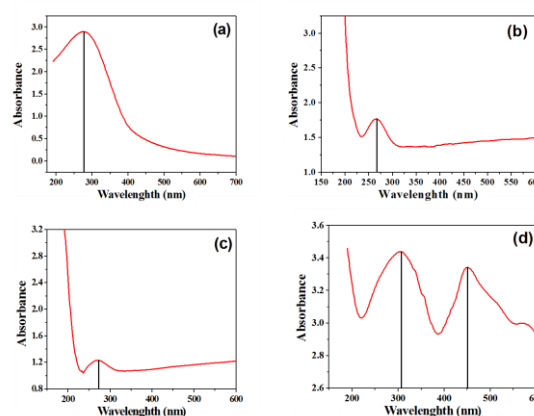


Figure 5. UV-Visible spectra of (a) pure TiO₂ (b) pure PPy (c) PPy/TiO₂ and (d) PPy/TiO₂/GO nanocomposites.

Determination of optical band gap of resulting composites

The band gap of polypyrrole TiO₂, polypyrrole, polypyrrole/TiO₂ and polypyrrole/TiO₂/GO were determined from absorption spectra and Tauc relation (Eqn. 1)

$$\alpha h\nu = B(h\nu - E_{\text{gap}})^m \dots\dots(1)$$

where α is the absorption coefficient, $h\nu$ is the photon energy, and $m = 1/2$ for direct band gap material. Ghobadi [35-37] described a direct method for fitting and determination of band gap using Tauc relation. After substitutions in Eqn. (1), we can write that Eqn. (2):

$$\alpha(\lambda) = B(hc)^{m-1} \lambda \left(\frac{1}{\lambda} - \frac{1}{\lambda_g} \right)^m \dots\dots\dots(2)$$

where λ_g , h , and c are wavelengths corresponding to the optical band gap, Planck's constant, and velocity of light, respectively. Using the Beer-Lambert's law, it is possible to rewrite Equation 2 as follows:

$$\text{Abs}(\lambda) = B_1 \lambda \left(\frac{1}{\lambda} - \frac{1}{\lambda_g} \right)^m + B_2 \dots\dots\dots(3)$$

where $B_1 = \frac{1}{4} B hc \delta P m$ and B_2 is a constant which take into account the reflection. Using Equation 5, one can calculate the optical band gap by an absorbance spectrum fitting method without any need to the film thickness. Thus the value of band gap, in electron volt, can be calculated from the parameter λ_g using $E_{\text{gap}} = \frac{1239.83}{\lambda_g}$; in other words, the value of λ_g can be extrapolating the linear of the $\text{Abs} \delta P \lambda$ vs. $1/\lambda$ curve at $\text{Abs} \delta P \lambda = 0$. By using the least squares technique, it was observed that the best fitting occurs for $m = 1/2$. Extrapolating the straight-line portion of the plots shown in Figure 1 to zero $\text{Abs} = \lambda P$ gives the corresponding E_{gap} (eV) values. The dependence of the optical gap on the deposition time for as-deposited thin films is shown in Figure 1 and Table 1. It is obvious that the optical gap is decreased by increasing the deposition time because with increasing deposition time, the size of the particles grows and the energy band gap decreases.

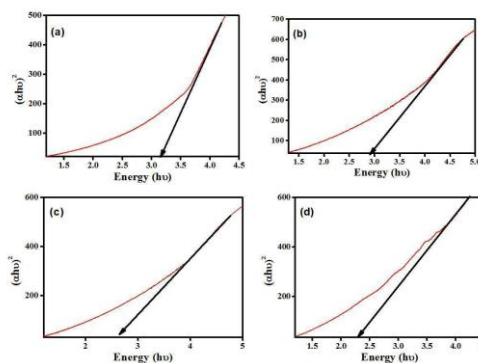


Figure 6. Band Gap energy of (a) pure TiO₂ (b) pure PPy (c) PPy/TiO₂ and (d) PPy/TiO₂/GO nanocomposites.

Fluorescence Spectra

The fluorescence spectra of pure TiO₂, pure PPy, PPy/TiO₂, PPy/TiO₂/GO nanocomposites are shown in Figure 7. The fluorescence of nanocomposites can be described in terms of semiconductor band theory. Upon photoexcitation of a conjugated polymer, the electrons from the valence band are excited to the conduction band and then migrated along the polymer backbone. The excited electron and the oppositely charged hole attract one another. When the excited electron combines with the hole a photon is emitted and it is known as fluorescence. [38]

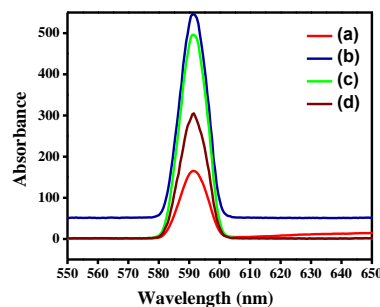


Figure 7. Fluorescence spectra of (a) pure PPy, (b) pure TiO₂, (c) PPy/TiO₂ and (d) PPy/TiO₂/GO nanocomposites.

IV. CONCLUSION

Conducting PPy/TiO₂ nanocomposites in HCl solution were successfully prepared by one-step in situ chemical oxidative polymerization of pyrrole using FeCl₃ as oxidant in the presence of ultra fine grade powder of anatase nano-TiO₂ particles cooled in

an ice bath. The obtained results from XRD, FT-IR, TGA and SEM data confirmed that TiO₂ nanoparticles are encapsulated by PPy. Electrical conductivity measurements indicate that the conductivity of nanocomposites at low TiO₂ content is much higher than that of neat PPy, while with the increasing contents of TiO₂, the conductivity shows an orderly decrease. TGA investigation shows that thermal stability of PPy/TiO₂ nanocomposites is higher in comparison with pure PPy. SEM study shows that TiO₂ nanoparticles have a strong effect on the morphology of PPy/TiO₂ nanocomposites. This employed method is very simple and inexpensive, and it can be easily applied industrially.

V. REFERENCES

- [1]. Fei Gao, Xianhui Hou, Aolan Wang, Guangwen Chu, Wei Wu, Jianfeng Chen, Haikui Zou, Preparation of polypyrrole/ TiO₂ nanocomposites with enhanced photocatalytic performance, *Particuology*, 26, 2016, 73-78.
- [2]. Mohd Omaish Ansari, Mohammad Mansoob Khan, Sajid Ali Ansari, Moo Hwan Cho, Polythiophene nanocomposites for photodegradation applications: Past, present and future, *Journal of Saudi Chemical Society*, 19, 2015, 494-504.
- [3]. Qizhao Wang, Longhui Zheng, Yutao Chen, Jiafeng Fan, Haohao Huang, Bitao Su, Synthesis and characterization of novel PPy/Bi₂O₂CO₃ composite with improved photocatalytic activity for degradation of Rhodamine-B, *Journal of Alloys and Compounds*, 637, 2015, 127-132.
- [4]. Desong Wang, Yanhong Wang, Xueyan Li, Qingzhi Luo, Jing An, Jianxia Yue, Sunlight photocatalytic activity of PPy- TiO₂ nanocomposites prepared by 'in situ' method, *Catalysis Communications*, 9, 2008, 1162-1166.
- [5]. Laura Peponi, Debora Puglia, Luigi Torre, Luca Valentini, José M. Kenny, Processing of nanostructured polymers and advanced polymeric based nanocomposites, *Materials Science and Engineering: R: Reports*, 85, 2014, 1-46.
- [6]. C. Piewnuan, J. Wootthikanokkhan, P. Ngaotrakanwivat, V. Meeyoo, S. Chiarakorn, Preparation of TiO₂/(TiO₂-V₂O₅)/polypyrrole nanocomposites and a study on catalytic activities of the hybrid materials under UV/Visible light and in the dark, *Superlattices and Microstructures*, 75, 2014, 105-117.
- [7]. Shuna Gu, Bing Li, Chongjun Zhao, Yunlong Xu, Xiuzhen Qian, Guorong Chen, Preparation and characterization of visible light-driven AgCl/PPy photocatalyst, *Journal of Alloys and Compounds*, 509, 2011, 5677-5682.
- [8]. Fang Deng, Yuexiang Li, Xubiao Luo, Lixia Yang, Xinman Tu, Preparation of conductive polypyrrole/TiO₂ nanocomposites, *Colloids and Surfaces A: Physicochemical and Engineering Aspects*, 395, 2012, 183-189.
- [9]. Yang Cheng, Fang Gao, Liang An, Xiaomin Li, Guanghui Wang, Different combinations of Fe₃O₄ microsphere, Polypyrrole and silver as core-shell nanocomposites for adsorption and photocatalytic application, *Advanced Powder Technology*, 25, 2014, 1600-1607.
- [10]. Syed Kazim Moosvi, Kowsar Majid, Tabassum Ara, Synthesis and characterization of PTP/Fe(CN)₃(dien)]·H₂O nanocomposites; study of electrical, thermal and photocatalytic properties, *Chemical Physics*, 478, 2016, 110-117.
- [11]. Ufana Riaz, S.M. Ashraf, Jyoti Kashyap, Enhancement of photocatalytic properties of transitional metal oxides using conducting polymers: A mini review, *Materials Research Bulletin*, 71, 2015, 75-90.
- [12]. Prawit Nuengmatcha, Saksit Chanthai, Ratana Mahachai, Won-Chun Oh, Visible light-driven photocatalytic degradation of rhodamine B and industrial dyes (texbrite BAC-L and texbrite NFW-L) by ZnO-Graphene-TiO₂ composite, *Journal of Environmental Chemical Engineering*, 4, 2016, 2170-2177.

- [13]. B.A. Rozenberg, R. Tenne, Polymer-assisted fabrication of nanoparticles and nanocomposites, *Progress in Polymer Science*, 33, 2008, 40-112.
- [14]. Farid A. Harraz, Adel A. Ismail, S.A. Al-Sayari, A. Al-Hajry, Novel α -Fe₂O₃/polypyrrole nanocomposites with enhanced photocatalytic performance, *Journal of Photochemistry and Photobiology A: Chemistry*, 299, 2015, 18-24.
- [15]. Mohammad Shahadat, Tjoon Tow Teng, Mohd. Rafatullah, Mohd. Arshad, Titanium-based nanocomposites materials: A review of recent advances and perspectives, *Colloids and Surfaces B: Biointerfaces*, 126, 2015, 121-137.
- [16]. Habib Ullah, Asif Ali Tahir, Tapas K. Mallick, Polypyrrole/TiO₂ composites for the application of photocatalysis, *Sensors and Actuators B: Chemical*, In Press, Corrected Proof, Available online 6 October 2016.
- [17]. Annamalai Pratheep Kumar, Dilip Depan, Namrata Singh Tomer, Raj Pal Singh, Nanoscale particles for polymer degradation and stabilization—Trends and future perspectives, *Progress in Polymer Science*, 34, 2009, 479-515.
- [18]. Kakarla Raghava Reddy, Mahbub Hassan, Vincent G. Gomes, Hybrid nanostructures based on titanium dioxide for enhanced photocatalysis, *Applied Catalysis A: General*, 489, 2015, 1-16.
- [19]. C. Janáky, K. Rajeshwar, The role of (photo) electrochemistry in the rational design of hybrid conducting polymer/semiconductor assemblies: From fundamental concepts to practical applications, *Progress in Polymer Science*, 43 2015, 96-135.
- [20]. Shu Zhang, Qingyun Chen, Yunhai Wang, Liejin Guo, Synthesis and photoactivity of CdS photocatalysts modified by polypyrrole, *International Journal of Hydrogen Energy*, 37, 2012, 13030-13036.
- [21]. Desong Wang, Cai Bao, Qingzhi Luo, Rong Yin, Xueyan Li, Jing An, Zexuan Xu, Improved visible-light photocatalytic activity and anti-photocorrosion of CdS nanoparticles surface-modified by conjugated derivatives from polyvinyl chloride, *Journal of Environmental Chemical Engineering*, 3, 2015, 1578-1585.
- [22]. Fang Wang, Shixiong Min, Yuqi Han, Lei Feng, Visible-light-induced photocatalytic degradation of methylene blue with polyaniline-sensitized composite photocatalysts, *Superlattices and Microstructures*, 48, 2010, 170-180
- [23]. Ericleiton R. Macedo, Patrícia S. Oliveira, Helinando P. de Oliveira, Synthesis and characterization of branched polypyrrole/titanium dioxide photocatalysts, *Journal of Photochemistry and Photobiology A: Chemistry*, 307-308, 2015, 108-114
- [24]. Zilin Ni, Yanjuan Sun, Yuxin Zhang, Fan Dong, Fabrication, modification and application of (BiO)₂CO₃-based photocatalysts: A review, *Applied Surface Science*, 365, 2016, 314-335.
- [25]. Hatice Ozkazanc, Sibel Zor, Electrochemical synthesis of polypyrrole (PPy) and PPy/metal composites on copper electrode and investigation of their anticorrosive properties, *Progress in Organic Coatings*, 76, 2013, 720-728.
- [26]. Sedlacík, M., Mrlík, M., Pavlínek, V., Sáha, P., & Quadrat, O.. Electrorheological properties of suspensions of hollow globular titanium oxide/polypyrrole particles. *Colloid and Polymer Science*, 290, 2012, 41-48.
- [27]. Serpone, N., & Emeline, A. Semiconductor photocatalysis past, present, and future outlook. *The Journal of Physical Chemistry Letters*, 3, 2012, 673-677.
- [28]. Sun, L., Shi, Y., Li, B., Li, X., & Wang, Y. Preparation and characterization of polypyrrole/TiO₂ nanocomposites by reverse microemulsion polymerization and its photocatalytic activity for the degradation of methyl orange under natural light. *Polymer Composites*, 34, 2013, 1076-1080.
- [29]. Tai, H., Jiang, Y., Xie, G., Yu, J., & Zhao, M. Self-assembly of TiO₂/polypyrrole nanocomposite ultrathin films and application

- for an NH₃ gas sensor. *International Journal of Environmental Analytical Chemistry*, 87, 2007, 539-551.
- [30]. Thompson, T. L., & Yates, J. T. Surface science studies of the photoactivation of TiO₂ new photochemical processes. *Chemical Reviews*, 106, 2006, 4428-4453.
- [31]. Wang, B., Li, C., Pang, J., Qing, X., Zhai, J., & Li, Q. Novel polypyrrole-sensitized hollow TiO₂/fly ash cenospheres: Synthesis, characterization, and photocatalytic ability under visible light. *Applied Surface Science*, 258, 2012, 9989-9996.
- [32]. Wang, D., Wang, Y., Li, X., Luo, Q., An, J., & Yue, J. Sunlight photocatalytic activity of polypyrrole-TiO₂ nanocomposites prepared by 'in situ' method. *Catalysis Communications*, 9, 2008, 1162-1166.
- [33]. Wang, Q., Wu, W., Chen, J., Chu, G., Ma, K., & Zou, H. Novel synthesis of ZnPc/TiO₂ composite particles and carbon dioxide photocatalytic reduction efficiency study under simulated solar radiation conditions. *Colloids and Surfaces A: Physicochemical and Engineering Aspects*, 409, 2012, 118-125.
- [34]. Nader Ghobadi, Band gap determination using absorption spectrum fitting procedure, *International Nano Letters* 2013, 3:2.
- [35]. Yang, Y., Wen, J., Wei, J., Xiong, R., Shi, J., & Pan, C. Polypyrrole-decorated AgTiO₂ nanofibers exhibiting enhanced photocatalytic activity under visible-light illumination. *ACS Applied Materials & Interfaces*, 2013, 6201-6207.
- [36]. Woan, K., Pyrgiotakis, G., & Sigmund, W. Photocatalytic carbon-nanotube/TiO₂ composites. *Advanced Materials*, 21, 2009, 2233-2239.
- [37]. Xu, S., Zhu, Y., Jiang, L., & Dan, Y. Visible light induced photocatalytic degradation of methyl orange by polythiophene/TiO₂ composite particles. *Water, Air, & Soil Pollution*, 213, 2010, 151-159.
- [38]. Yan, H., Zhang, L., Shen, J., Chen, Z., Shi, G., & Zhang, B. Synthesis, property and field-emission behaviour of amorphous polypyrrole n